Hindawi Publishing Corporation
EURASIP Journal on Wireless Communications and Networking
Volume 2009, Article ID 940584, 12 pages
doi:10.1155/2009/940584

Research Article

Optimal Channel Width Adaptation, Logical Topology Design, and Routing in Wireless Mesh Networks

Li Li and Chunyuan Zhang

College of Computer Science, National University of Defense Technology, Changsha, Hunan, China

Correspondence should be addressed to Li Li, lili_wz@188.com

Received 23 December 2008; Accepted 16 March 2009

Recommended by Ingrid Moerman

Radio frequency spectrum is a finite and scarce resource. How to efficiently use the spectrum resource is one of the fundamental issues for multi-radio multi-channel wireless mesh networks. However, past research efforts that attempt to exploit multiple channels always assume channels of fixed predetermined width, which prohibits the further effective use of the spectrum resource. In this paper, we address how to optimally adapt channel width to more efficiently utilize the spectrum in IEEE802.11-based multi-radio multi-channel mesh networks. We mathematically formulate the channel width adaptation, logical topology design, and routing as a joint mixed 0-1 integer linear optimization problem, and we also propose our heuristic assignment algorithm. Simulation results show that our method can significantly improve spectrum use efficiency and network performance.

1. Introduction

Wireless mesh networks (WMNs) consist of a multihop backbone of mesh routers which collect and relay the traffic generated by mesh clients [1]. A fundamental obstacle to building large-scale multihop wireless networks is the insufficient network capacity when route lengths and network density increase due to the limited spectrum shared in the neighborhood [2]. The use of multiple radios which tuned into different channels can significantly improve the network capacity by employing concurrent transmissions under different channels, and that motivates the development of new protocols for multi-radio multi-channel (MR-MC) mesh networks.

Radio frequency spectrum is a finite and scarce resource. How to efficiently use the spectrum resource is one of the fundamental issues in MR-MC mesh networks. In order to eliminate interference, traditional spectrum management schemes always partition the available spectrum into multiple wireless channels. A wireless channel is a continuous portion of the frequency spectrum over which radio can transmit or receive its signals. Channels can be characterized by the center frequency and channel width. For example, as Figure 1 shows, the 2.4 GHz band that 802.11 b/g [3] standards operate on is split into eleven channels of 22 MHz-width, where the center frequencies of adjacent channels are spaced by 5 MHz apart. So among the eleven channels, only three are non-overlapped, namely, 1, 6, and 11. Due to the traditional static spectrum partition style, almost all past research work assume channels of fixed predetermined width. Recently some work [4–6] identified the inefficiency of the static spectrum partition style and began to explore the use of dynamic channel width adaptation.

The aim of spectrum assignment is to distribute the traffic load across the spectrum as evenly as possible. Fixed-width channels can support uniformly distributed traffic very well. But when the traffic distribution is skewed, the use of fixed-width channels will be suboptimal and prohibit the more effectively utilizing the spectrum resource. Let us take Figure 2 as an example. Figure 2 shows a chain topology where adjacent nodes are 200 m apart. Each node is assumed to be equipped with two radio interfaces. The effective transmission range is 250 m, and the interfering range is 550 m. The IEEE802.11 standard with RTS/CTS/DATA/ACK four-way handshake is assumed to be used. So two links within 3-hop range will conflict with each other when they use the same channel.

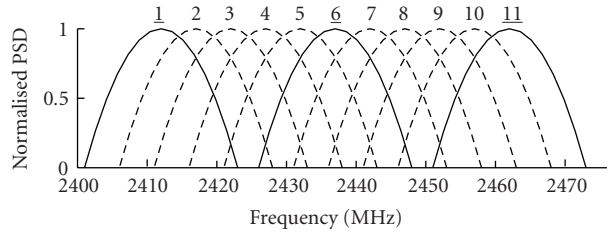

Figure 1: Available eleven channels of fixed predetermined width defined in 802.11 b/g standards.

Each of the nodes from 1 to 9 is assumed to generate a flow of same throughput U towards the gateway, node 10. Intermediate nodes act as traffic generators as well as traffic routers at the same time. So different links carry different traffic loads. In Figure 2(a), the number above each link indicates the expected load on the link. For example, link (5, 6) has a load of $5U$ since it forwards flows originating from nodes 1 to 4 and the flow generated by node 5 itself. Obviously, the bottleneck collision domain consists of links (6, 7), (7, 8), (8, 9), and (9, 10), and hence limits the throughput U for each flow.

We assume the total available spectrum is 60 MHz wide, and each 1 MHz spectrum can deliver 1 Mbps data rate. Here we consider static spectrum assignment scheme, that is, channels are assigned to interfaces/links on a long-term basis. In Figure 2(b), we first investigate the case that the whole available spectrum is divided into three 20 MHz-wide non-overlapped channels. So at least two links among (6, 7), (7, 8), (8, 9), and (9, 10) will be assigned to the same channel. As Figure 2(b) shows, the optimal scheme is to assign a same channel to link (6, 7) and (7, 8), and assign the other two channels to (8, 9) and (9, 10), respectively. Under this scheme, links (6, 7) and (7, 8) become the bottleneck and every flow can obtain the throughput U up to 20/13 Mbps. In Figure 2(c), we then investigate another case that four 15 MHz-wide channels are available. Now no two links will interfere with each other. Obviously, the bottleneck link is (9, 10), and every flow can get the throughput U up to 5/3 Mbps, which is better than the previous case.

Note that flows could not benefit from the enhanced capacity without first reducing the bottleneck wireless links. By optimally adjusting channel width for every link, we can get the most efficient spectrum assignment scheme as Figure 2(d) shows. The spectrum that every link uses exactly matches its traffic load. Now the throughput U for every flow can get up to 2 Mbps. Compared with the previous two fixed-width assignment schemes, channel width adaptation can improve the network performance by 30% and 20%, respectively.

Motivated by the above example, we strongly advocate the channel width adaptable network architecture. Briefly speaking, the advantages of channel width adaptation are two-fold. On one hand, we can distribute the traffic as evenly as possible across the spectrum in a fine granularity to achieve channel load balance. On the other hand, in a scenario with many interfering links, by "creating" more small-width orthogonal channels, we can greatly reduce the phenomena of contention and collision, and therefore improve throughput as a result of fewer back-offs and reduced interference. Another motivation for the channel width adaptable network architecture is the recent open spectrum effort [7] made by the spectrum regulation authority such as FCC. Because of the variable widths of "white space" unoccupied by licensed users, we believe channel width adaptation will become one of the most important functions for cognitive radio networks in future open spectrum environment.

The characteristic of wireless mesh networks [1] makes it attractive and feasible to use channel width adaptation. First, in WMN, each mesh router aggregates traffic flows for a large number of mobile clients, and therefore the aggregate traffic load changes infrequently, which offers the predictability for assigning channel width in term of traffic pattern and permits capacity optimization based on estimated traffic demand. Second, mesh nodes (or routers) are usually static and have no power constraints, and therefore physical topology changes only occur due to occasional node failures, or addition of new nodes. Thus channel width adaptation can be implemented on a long-term basis without requiring resynchronization of interfaces for every packet. Third, some mesh routers are used as gateways to connect the wired network, and most traffic is between the mesh clients and the wired networks through these gateways. So the traffic distribution in WMN is typically skewed as the example in Figure 2 shows: gateway nodes would form the bottlenecks since more and more flows contend for the bandwidth as they are forwarded closer to gateways. Channel width adaptation will surely promise great flexibility to accommodate such skewed traffic distribution.

In this paper, we address how to optimally adapt channel width in IEEE802.11-based multi-radio multi-channel wireless mesh networks. We mathematically formulate the channel width adaptation, logical topology design, and routing as a joint optimization problem. Our mathematical formulation not only takes into account the issues in traditional MR-MC mesh networks, such as the number of available interfaces, the interference constraints, and the expected traffic load, but also determines at what center frequency and how wide a spectrum band an interface should use. Extensive simulations show that channel width adaptation can significantly improve spectrum use efficiency and network performance.

The rest of the paper is organized as follows. Section 2 reviews the related work. Section 3 presents the network

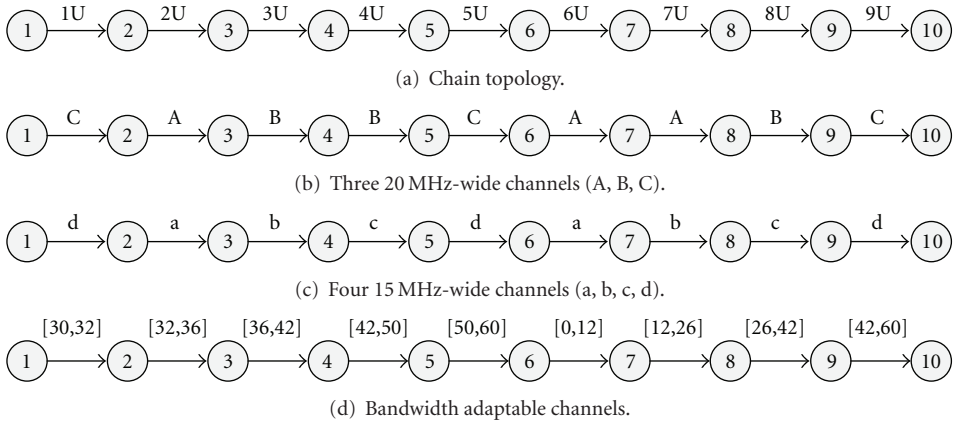

(a) Chain topology.

(b) Three 20 MHz-wide channels (A, B, C).

(c) Four 15 MHz-wide channels (a, b, c, d).

(d) Bandwidth adaptable channels.

Figure 2: Scenarios illustrating the inefficiency of using channels with fixed predetermined width. In Figure 2(d), above each link, $[x, y]$ denotes the frequency interval ranging from x MHz to y MHz which is assigned to that link.

model and Section 4 formulates the problem as a mixed integer nonlinear programming. In Section 5, we convert the problem into an equivalent mixed 0–1 integer linear programming and propose a suboptimal heuristic solution. Simulation results are presented in Section 6, and Section 7 concludes this paper.

2. Related Work

There exists a wide range of related works aiming to design efficient channel assignment algorithms for multi-radio multi-channel mesh networks.

Raniwala proposed a static centralized channel assignment algorithm in [8], and in [9], an improved distributed channel assignment algorithm with load-balance routing was proposed. In [10], channels are allocated so as to minimize the maximum number of interfering links within each neighborhood, subject to the constraint that the logical topology graph should be K-connected. In [11], Kyasanur and Vaidya proposed a hybrid channel assignment strategy, easing the channel synchronization. Literature [12] proposed a routing protocol which incorporates a routing metric taking account of both the loss rate and the channel diversity of links along the path. All the above algorithms are based on heuristic methods, not mathematical formulations.

Many other works formulate the problem as a joint mathematical programming. In [13], Alicherry et al. formulated a joint channel assignment and routing problem for the MR-MC network, with the aim of maximizing network throughput subject to the proportional fairness constraints. Literature [14] provided necessary conditions of the feasibility of rate vectors and used a fast primal-dual algorithm to derive upper bounds of the achievable throughput. In [15], two models that maximize the number of logical links that can be active simultaneously were proposed, subject to interference constraints. In [16], the MR-MC mesh architecture called *TiMesh* was proposed, which formulates the logical topology control and interface assignment as a joint optimization problem. All the above works assume channels of fixed predetermined width.

Literature [17] proposed a spectrum sharing model for cognitive radio networks based on mixed integer nonlinear programming with the objective of minimizing the required network-wide spectrum resource for a set of user sessions, and developed a near-optimal algorithm based on the sequential fixing procedure. It was mentioned in [17] that equal band division of the spectrum yields suboptimal performance and thus it calculated an optimal global band partition. The significant difference between [17] and ours is that [17] only tries to obtain a global spectrum regulation for the whole networks so that all nodes can use only one spectrum partition style, while in our architecture we can adjust channel width flexibly across nodes (i.e., different nodes may use different spectrum partition styles), which offers further flexibility.

Literature [4] first systematically studied the issues of channel width adaptation. Using commodity 802.11 hardware, it gave a method to generate signals of different channel widths by changing the frequency of the reference clock that drives the frequency synthesizer of the radio front end circuitry, which can be configured dynamically purely in software. And through detailed measurements in controlled environments, it then preliminarily identified several benefits of channel width adaptation in many metrics of wireless networks: range and connectivity, power consumption, network capacity and fairness. Finally, it proposed a channel width adaptation algorithm, called *SampleWidth*, for two communicating nodes. In [5], three centralized channel width adaptation algorithms using ILP, LP-based packing and greedy raising were proposed for WLAN to improve network capacity and per-client fairness. Literature [6] designed a dynamic channel width allocation protocol called *b-SMART* for cognitive radio networks. Using the concept of time-spectrum block, the spectrum allocation is reduced into the problem of packing time-spectrum blocks into a two-dimensional time-frequency space. The algorithm of [6] resided in the MAC layer and required advanced radio hardware with fast switching and channel width adaptation ability on a packet-by-packet basis, significantly increasing the signaling

overhead due to the fast coordination. In our architecture, channel width adaptation is on a long-term basis (e.g., every several minutes or hours), hence does not require resynchronization of interfaces for every packet and the modification of IEEE802.11 MAC protocols, and thus becomes more practical for current available commercial hardware and easy to be used in wireless backbone mesh networks.

3. Network Model and Problem Formulation

We model the wireless mesh networks by an undirected graph $G(V, E)$, where V denotes the set of all vertices and E denotes the set of all edges. Each vertex $n \in V$ represents a wireless mesh node equipped with K_n network interface cards, and we use n_p to denote the pth interface of node n, where $p = 1, 2, \ldots, K_n$. For any two nodes $n, m \in V$, if node n is within the communication range of node m, then there is a physical link $(n, m) \in E$ between n and m. We assume that all links are bidirectional.

Note that every node has multiple interfaces which can be tuned into different portions of the spectrum, so there may exist zero, one, or more logical links between two neighboring nodes. Then based on the graph G, we develop another radio-based graph $G'(V', E')$, where $V' = \{n_p \mid n \in V,\ p = 1, \ldots, K_n\}$ and $E' = \{(n_p, m_q) \mid (n, m) \in E;\ p = 1, \ldots, K_n; q = 1, \ldots, K_m\}$. We call the links in E physical links and the links in E' logical links. The logical link (n_p, m_q) will exist in the final logical topology after spectrum allocation if and only if the pth interface of node n and the qth interface of node m operate on the same portion of spectrum.

We assume that each interface can only be tuned into a contiguous segment of the available spectrum. Due to the hardware constraint, the possible channel widths are some discrete values in the range of $[b_{\min}, b_{\max}]$. So it is reasonable to partition the whole available spectrum into a series of sequential small-width non-overlapped spectrum blocks. We denote the set of blocks as $\mathcal{F}$ and the size of a spectrum block as ω. So the problem of channel width adaptation is equivalent to the contiguous spectrum blocks allocation. For example, in Figure 2, we can set $\omega = 2$ MHz, and the whole available 60 MHz-wide spectrum will be divided into 30 blocks. Link $l_{9,10}$ will be assigned the block 22 to block 30 and link $l_{8,9}$ will be assigned the block 14 to block 21 in the scheme of Figure 2(d). According to Shannon's capacity theorem [18], we also reasonably assume that the achievable data rate is proportional to the assigned channel width, that is, the number of spectrum blocks allocated, and we let c_{unit} be the link-layer data rate that one spectrum block can deliver.

We use $\text{Inf}(n, m) \subset E$ to denote the set of physical links that are in the interference range of link (n, m). Note link $(u, v) \in \text{Inf}(n, m)$ also indicates $(n, m) \in \text{Inf}(u, v)$. We assume that the non-overlapped spectrum bands are orthogonal, that is, simultaneous use of non-overlapped spectrum blocks in the same area will not interfere. Though there may exist adjacent channel interference due to improper signal processing at the wireless cards and poor filter characteristics, we believe with the advance of radio technology, adjacent channel interference can be avoided to a large extent, and even partially overlapped channels with variable width can be further exploited in the future.

We assume that a reasonable statistical traffic demand matrix T is available. And let $L_{s,d}$ denote the traffic demand between the source and destination pair $(s, d) \in T$, where $s, d \in V$. Our aim is to design schemes to maximize the capacity of the network. The network capacity cannot be simply measured by the total throughput of all traffic flows. Optimizing such metric may lead to starvation of some flows which originate far from gateways. We therefore need to consider some fairness constraints. Similar to [13], we adopt the proportional fairness, that is, the same portion of traffic demand will be satisfied for every flow $(s, d) \in T$. So we want to find the schemes that $\lambda L_{s,d}$ traffic of every flow $(s, d) \in T$ can be routed for the largest possible λ. Other kinds of fairness constraint like the lexicographical max-min fairness [19] can also be adopted.

It is suboptimal to assigning spectrum without considering the logical topology control and traffic routing. So in our work, the following three aspects will be jointly considered:

(1) logical topology design: which logical links in E' will exist in the final topology?

(2) spectrum block assignment: how to efficiently assign contiguous spectrum blocks to each interface?

(3) routing: how to optimally route the traffic to achieve load balance across different links?

4. Joint Topology Design, Spectrum Assignment, and Routing

In this section, we describe how we formulate the logical topology design, contiguous spectrum block assignment, and routing as a joint optimization problem. We will use the letter like $\bar{l}$ to denote a vector, and use l^i to denote the ith element of the vector $\bar{l}$.

4.1. Contiguous Spectrum Block Allocation. For any radio interface n_p of node n ($n \in V$, $p = 1, \ldots, K_n$), we define a $|\mathcal{F}| \times 1$ spectrum block assignment vector $\bar{a}_{n_p}$ as follows:

$$a^i_{n_p} = \begin{cases} 1, & \text{if spectrum block } i \text{ is assigned to radio } n_p, \\ 0, & \text{otherwise,} \end{cases} \tag{1}$$

where $a^i_{n_p}$ is the ith element of $\bar{a}_{n_p}$. For example, in Figure 2(d), assuming node 9 uses its 2nd interface to communicate with node 10, we have $a^{22}_{9_2} = a^{23}_{9_2} = \cdots = a^{30}_{9_2} = 1$ while the other elements are equal to zero.

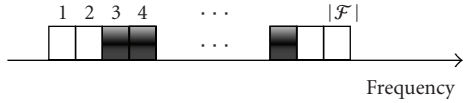

$\overline{a}_{n_p}$ [0, 0, 1, 1, ... ,1, 0, 0]^T
$\overline{x}_{n_p}$ [0, 0, 1, 0, ... ,0, 0, 0]^T
$\overline{y}_{n_p}$ [0, 0, 0, 0, ... ,1, 0, 0]^T

FIGURE 3: Illustration for vectors $\overline{a}_{n_p}$, $\overline{x}_{n_p}$, and $\overline{y}_{n_p}$.

In order to characterize the contiguous spectrum block allocation, we then introduce two $|\mathcal{F}| \times 1$ auxiliary binary vectors $\overline{x}_{n_p}$ and $\overline{y}_{n_p}$ for $\overline{a}_{n_p}$ as follows:

$$x^i_{n_p} = \begin{cases} 1, & \text{if } a^i_{n_p} = 1 \text{ and } a^j_{n_p} = 0,\ j = 1, 2, \ldots, i-1, \\ 0, & \text{otherwise,} \end{cases}$$

$$y^i_{n_p} = \begin{cases} 1, & \text{if } a^i_{n_p} = 1 \text{ and } a^j_{n_p} = 0,\ j = i+1, \ldots, |\mathcal{F}|, \\ 0, & \text{otherwise.} \end{cases} \tag{2}$$

Figure 3 illustrates a vector $\overline{a}_{n_p}$ and the corresponding vectors $\overline{x}_{n_p}$ and $\overline{y}_{n_p}$. We can find the elements valued 1 of $\overline{x}_{n_p}$ and $\overline{y}_{n_p}$ indicate the lower and upper end of spectrum blocks assigned to the radio interface n_p, respectively. Obviously every valid $\overline{a}_{n_p}$ corresponds to only one form of $\overline{x}_{n_p}$ and $\overline{y}_{n_p}$.

$\overline{x}_{n_p}$ and $\overline{y}_{n_p}$ should satisfy

$$x^i_{n_p},\ y^i_{n_p} \in \{0, 1\}, \quad i = 1, 2, \ldots, |\mathcal{F}|, \tag{3}$$

$$\sum_{i=1}^{|\mathcal{F}|} x^i_{n_p} = \sum_{i=1}^{|\mathcal{F}|} y^i_{n_p} \le 1, \tag{4}$$

$$\sum_{i=1}^{|\mathcal{F}|} 2^i x^i_{n_p} \le \sum_{i=1}^{|\mathcal{F}|} 2^i y^i_{n_p}, \tag{5}$$

$$\sum_{i=1}^{|\mathcal{F}|} 2^i y^i_{n_p} \le \sum_{i=1}^{|\mathcal{F}|} 2^i x^i_{n_{p+1}}, \quad 1 \le p \le K_n - 1. \tag{6}$$

It is possible some radio interfaces do not take part in any communication, so in this case, in constraint (4), $\sum_{i=1}^{|\mathcal{F}|} x^i_{n_p}$ and $\sum_{i=1}^{|\mathcal{F}|} y^i_{n_p}$ can be zero. Constraint (5) means that the lower end of the spectrum segment should locate lower than the upper end. And in constraint (6), without loss of generality, we further assume that the spectrum segment that interface n_p uses locates lower than that of n_{p+1}. Now using $\overline{x}_{n_p}$ and $\overline{y}_{n_p}$, we can redefine $\overline{a}_{n_p}$ as follows.

$$a^i_{n_p} = \sum_{j=1}^{i} x^j_{n_p} \times \sum_{j=i}^{|\mathcal{F}|} y^j_{n_p}, \quad i = 1, 2, \ldots, |\mathcal{F}|. \tag{7}$$

Which means for the element $a^i_{n_p}$, if it resides between the lower end and the upper end, it will be equal to 1, otherwise 0.

When interface n_p participates some communication, its channel width should be in the range of $[b_{\min}, b_{\max}]$, so the total spectrum blocks that it can utilizes should be in the range between $b_{\min}/\omega$ and $b_{\max}/\omega$, that is,

$$\frac{b_{\min}}{\omega} \sum_{i=1}^{|\mathcal{F}|} x^i_{n_p} \le \sum_{i=1}^{|\mathcal{F}|} a^i_{n_p} \le \frac{b_{\max}}{\omega} \sum_{i=1}^{|\mathcal{F}|} x^i_{n_p}. \tag{8}$$

When we set $b_{\min} = b_{\max}$, our model will degenerate into the traditional multi-radio multi-channel networks using fixed-width channels.

Using the constraints (3) to (8), we can fully characterize the contiguous spectrum block allocation. Note we can treat $\overline{a}_{n_p}$ as continuous real vectors since we can infer $\overline{a}_{n_p}$ to be binary vectors from the above constraints.

4.2. Logical Topology Formulation. Vectors $\overline{x}_{n_p}$ and $\overline{y}_{n_p}$ (thus $\overline{a}_{n_p}$) can fully characterize the logical topology formulation. The link $(n_p, m_q) \in E'$ will exist in final logical topology only when the interfaces n_p and m_q operate on the same set of spectrum blocks. Then we use variable e_{n_p,m_q} to denote whether the logical link (n_p, m_q) will exist, that is,

$$e_{n_p,m_q} = \begin{cases} 1, & \text{if } \overline{a}_{n_p} = \overline{a}_{m_q}, \\ 0, & \text{otherwise.} \end{cases} \tag{9}$$

We can alternatively express e_{n_p,m_q} as follows:

$$0 \le 1 - e_{n_p,m_q} \le \sum_{i=1}^{|\mathcal{F}|} a^i_{n_p} \bigoplus a^i_{m_p}, \tag{10}$$

$$0 \le e_{n_p,m_q} \le 1 - a^i_{n_p} \bigoplus a^i_{m_q} \quad i = 1, \ldots, |\mathcal{F}|, \tag{11}$$

where $\bigoplus$ is the exclusive OR (XOR) operator. It is easy to verify the above correspondence. If there is some spectrum block i that interface n_p uses while m_q does not or m_q uses while n_p does not, that is, $a^i_{n_p} \bigoplus a^i_{m_q} = 1$, constraint (11) will imply that $e_{n_p,m_q} = 0$. Otherwise, $a^i_{n_p} \bigoplus a^i_{m_q} = 0$ for $i = 1, \ldots, |\mathcal{F}|$, constraint (10) will imply that $e_{n_p,m_q} = 1$. Note we can also treat e_{n_p,m_q} as continuous variables.

With e_{n_p,m_q} and $\overline{a}_{n_p}$, we can easily obtain the spectrum assignment vector $\overline{a}_{n_p,m_q}$ for any logical link $(n_p, m_q) \in E'$

$$a^i_{n_p,m_q} = e_{n_p,m_q} \times a^i_{n_p} \left(= e_{n_p,m_q} \times a^i_{m_q}\right), \quad i = 1, \ldots, |\mathcal{F}|. \tag{12}$$

And the channel width that link (n_p, m_q) uses is equal to $\omega \sum_{i=1}^{|\mathcal{F}|} a^i_{n_p,m_q}$.

4.3. Routing. In multihop WMNs, a source node may need a number of relay nodes to route the data traffic towards its destination node. We need to compute a network flow that associates with each logical link $(n_p, m_q) \in E'$ valued $f^{s,d}_{n_p,m_q}$, where $f^{s,d}_{n_p,m_q}$ denotes the traffic data rate for the source and destination pair (s, d) that is being routed via the logical link (n_p, m_q) in the direction from n_p to m_q, assuring the λ times

of the traffic load valued $L_{s,d}$ for every source and destination pair $(s,d) \in T$ can be routed.

The network flow should satisfy the following constraint: for all $n \in V$, for all $(s,d) \in T$

$$\sum_{m\in\{v|(n,v)\in E\}} \sum_{p=1}^{K_n}\sum_{q=1}^{K_m} \left(f^{s,d}_{n_p,m_q} - f^{s,d}_{m_q,n_p}\right) = \begin{cases} \lambda L_{s,d}, & \text{if } s = n, \\ -\lambda L_{s,d}, & \text{if } d = n, \\ 0, & \text{otherwise,} \end{cases} \tag{13}$$

which means if node n is the source of the flow, the net flow sent by node n should be equal to $\lambda l_{s,d}$. If node n is the destination of the flow, it should be equal to $-\lambda l_{s,d}$. For the intermediate relay node, the net flow should be 0. Note a feasible network flow also guarantees that the final logical topology is connected.

The above constraint is only valid for the multi-path routing, which can take advantage of load balancing. We also investigate the single-path routing, which needs more constraints besides (13). We define a binary routing variable $r^{s,d}_{n_p,m_q}$ for all $(n_p,m_q) \in E'$ and for all $(s,d) \in T$. The variable $r^{s,d}_{n_p,m_q}$ will be equal to 1 if the flow from source s to destination d is only routed via the logical link (n_p,m_q) in the direction from n_p to m_q; otherwise it will be equal to 0. So $r^{s,d}_{n_p,m_q}$ should satisfy

$$r^{s,d}_{n_p,m_q} \in \{0,1\}, \tag{14}$$

$$\sum_{m\in\{v|(n,v)\in E\}} \sum_{p=1}^{K_n}\sum_{q=1}^{K_m} r^{s,d}_{n_p,m_q} \le 1 \quad \forall n \in V, \forall (s,d) \in T, \tag{15}$$

$$f^{s,d}_{n_p,m_q} = \lambda r^{s,d}_{n_p,m_q} L_{s,d} \quad \forall \left(n_p,m_q\right) \in E'. \tag{16}$$

Constraint (15) ensures only one path exists between any source and destination pair in T, and constraint (16) guarantees that the flow will be routed along the path.

4.4. Interference Issues. For any two logical links $(n_p,m_q) \in E'$ and $(u_h,v_l) \in E'$ that $(u,v) \in \mathrm{Inf}\,(n,m)$, we define interference indicator variable I_{n_p,m_q,u_h,v_l} as follows,

$$I_{n_p,m_q,u_h,v_l} = \begin{cases} 1, & \text{if } \exists i \in \{1,2,\ldots,|\mathcal{F}|\},\ a^i_{n_p,m_q} = a^i_{u_h,v_l} = 1 \\ 0, & \text{otherwise} \end{cases} \tag{17}$$

that is when these two logical links use overlapped spectrum blocks, they will interfere with each other ($I_{n_p,m_q,u_h,v_l} = 1$).

Similar to the variable e_{n_p,m_q}, we can express the correspondence among I_{n_p,m_q,u_h,v_l}, $\overline{a}_{n_p,m_q}$ and $\overline{a}_{u_h,v_l}$ with the following constraints:

$$a^i_{n_p,m_q} \times a^i_{u_h,v_l} \le I_{n_p,m_q,u_h,v_l} \le 1, \quad i = 1,\ldots,|\mathcal{F}|, \tag{18}$$

$$0 \le I_{n_p,m_q,u_h,v_l} \le \sum_{i=1}^{|\mathcal{F}|} a^i_{n_p,m_q} \times a^i_{u_h,v_l}. \tag{19}$$

4.5. Capacity Constraints. The fixed amount of spectrum provides limited capacity that will be shared among the links in interference range. First, we define a real variable u_{n_p,m_q} as the link utilization for every logical links $(n_p,m_q) \in E'$, that is, the fraction in one unit time that link (n_p,m_q) is active. Remember that we assume channel capacity is proportional to the number of spectrum blocks it used. So $u_{n,m}$ should satisfy the following constraints:

$$c_{\mathrm{unit}} \sum_{i=1}^{|\mathcal{F}|} a^i_{n_p,m_q} u_{n_p,m_q} = \sum_{(s,d)\in T} f^{s,d}_{n_p,m_q} + \sum_{(s,d)\in T} f^{s,d}_{m_q,n_p}, \tag{20}$$

$$0 \le u_{n_p,m_q} \le e_{n_p,m_q}. \tag{21}$$

The term on right-hand side of constraint (20) is the total traffic rate from all source and destination pairs that is routed over link (n_p,m_q), which is equal to the link utilization multiplies the channel capacity $c_{\mathrm{unit}} \sum_{i=1}^{|\mathcal{F}|} a^i_{n_p,m_q}$. Since $\sum_{i=1}^{|\mathcal{F}|} a^i_{n_p,m_q}$ can be 0 (when the logical link does not exist in the final logical topology, that is, $e_{n_p,m_q} = 0$), we use constraint (21) to set u_{n_p,m_q} to be 0 in that case.

Extending the sufficient condition for the existence of inference-free schedule of [13], we have, for any $(n_p,m_q) \in E'$,

$$u_{n_p,m_q} + \sum_{(u,v)\in \mathrm{Inf}\,(n,m)} \sum_{h=1}^{K_u}\sum_{l=1}^{K_v} u_{u_h,v_l} I_{n_p,m_q,u_h,v_l} \le 1 \tag{22}$$

which means that the total active time of logical link (n_p,m_q) and all other interfering links in one unit time can not exceed 1.

4.6. Objective Function. As stated before, our objective is to find the largest possible λ, that is,

$$\textbf{maximize } \lambda. \tag{23}$$

Now given the topology graph $G(V,E)$, the parameters ω, $b_{\min}, b_{\max}$, $\mathcal{F}$, K_n, c_{unit}, and $L_{s,d}$ for all source and destination pairs in T, we can state our problem formally using (3)-(23). However, note that many terms such as $\sum_{j=1}^{i} x^j_{n_p} \times \sum_{j=i}^{|\mathcal{F}|} y^j_{n_p}$ in (7), $a^i_{n_p} \bigoplus a^i_{m_q}$ in (10) and (11), and $a^i_{n_p,m_q} u_{n_p,m_q}$ in (20) are nonlinear. Even relaxing the binary constraints of (3) and (14), the problem is still nonconvex. So the above programming is a mixed-integer nonconvex program and generally it is not easy to be solved.

5. Solving the Problem

In this section, we first use some linearization techniques to convert the original mixed-integer nonlinear programming into a mixed-integer linear programming. Then we show how to choose the optimal solution with least interference. Finally we propose our heuristic MILP-based iterative local search algorithms.

5.1. Equivalent 0–1 Mixed-Integer Linear Programming. Thanks to some binary linearization techniques [20, 21], we can convert the above nonconvex programming into an equivalent mixed integer linear programming. Table 1 lists three methods that will be used in our work. In the table, the nonlinear constraint in column 1 can be equivalently replaced by the corresponding linear constraints of column 3. These linearization techniques are also used in [22] for partially overlapped channel assignment.

The validity of the above methods can be easily verified by enumerating all possible combinations of θ_1 and θ_2. We take $\tau = \theta_1 \bigoplus \theta_2$ as the example, where θ_1 and θ_2 are two binary variables. When $\theta_1 = \theta_2 = 0$, the first linear constraint $\theta_1 - \theta_2 \le \tau$ will imply $\tau \ge 0$, and the third linear constraint $\tau \le \theta_1 + \theta_2$ will imply $\tau \le 0$, so we can get $\tau = 0$. When $\theta_1 = 1, \theta_2 = 0$, or $\theta_1 = 0, \theta_2 = 1$, the first/second constraints will imply $\tau \ge 1$, and the third and the fourth constraints will imply $\tau \le 1$, so $\tau = 1$. Finally when $\theta_1 = \theta_2 = 1$, the first and the second constraint will imply $\tau \ge 0$, and the fourth constraint will imply $\tau \le 0$, and we can conclude that $\tau = 0$. So the four linear constraints are exactly equivalent to the original nonlinear constraint. And note we can treat τ as real variables. The other two methods can be verified in the similar way.

In the original programming of Section 4, $\overline{x}_{n_p}$, $\overline{y}_{n_p}$, and $r^{s,d}_{n_p,m_q}$ are explicitly declared binary vectors, while $\overline{a}_{n_p}$, $\overline{a}_{n_p,m_q}$, e_{n_p,m_q} and I_{n_p,m_q,u_h,v_l} can be directly or intermediately implied to be binary vectors or binary variables from $\overline{x}_{n_p}$ and $\overline{y}_{n_p}$. u_{n_p,m_q} is a non-negative real variable with an upper bound valued 1, and λ is also a non-negative real variable upper bounded by $|\mathcal{F}|c_{\text{unit}}/L_{s,d}$. So it is possible for us to convert all the nonlinear terms into linear ones. For example, for the nonlinear term $a^i_{n_p} \bigoplus a^i_{m_q}$ in (10) and (11), we can first introduce auxiliary variables $\tau^i_{n_p,m_q} = a^i_{n_p} \bigoplus a^i_{m_q}$ for all $(n_p, m_q) \in E'$, $i = 1, \ldots, |\mathcal{F}|$, and then replace the constraint (10) and (11) with the linear constraints as follows:

$$\begin{cases} 0 \le 1 - e_{n_p,m_q} \le \sum_{i=1}^{|\mathcal{F}|} a^i_{n_p} \bigoplus a^i_{m_q} \\ 0 \le e_{n_p,m_q} \le 1 - a^i_{n_p} \bigoplus a^i_{m_q} \quad i = 1, \ldots, |\mathcal{F}| \end{cases}$$

$$\Rightarrow \begin{cases} 0 \le 1 - e_{n_p,m_q} \le \sum_{i=1}^{|\mathcal{F}|} \tau^i_{n_p,m_q}, \\ 0 \le e_{n_p,m_q} \le 1 - \tau^i_{n_p,m_q}, \quad i = 1, \ldots, |\mathcal{F}|, \\ a^i_{n_p} - a^i_{m_q} \le \tau^i_{n_p,m_q} \le a^i_{n_p} + a^i_{m_q}, \quad i = 1, \ldots, |\mathcal{F}|, \\ a^i_{m_q} - a^i_{n_p} \le \tau^i_{n_p,m_q} \le 2 - a^i_{n_p} - a^i_{m_q}, \quad i = 1, \ldots, |\mathcal{F}|. \end{cases} \tag{24}$$

By applying the above three methods to convert all nonlinear constraints into linear ones, we will get a mixed 0-1 integer linear programming (which is called as MILP-1). The programming MILP-1 has $2|\mathcal{F}|\sum_{n\in\nu} K_n$ binary integer variables if we use multipath routing and additional $|T|\sum_{(n,m)\in E} K_n K_m$ binary integer variables if we use single path routing. We can use the traditional branch-and-bound algorithms [23] or use commercial software solver such as LINDO [24] and CPLEX [25] to solve the problem.

5.2. The Optimal Scheme with Least Interference. The solution of programming MILP-1 is a spectrum assignment scheme and a routing strategy that can maximize the value of λ among all feasible solutions. However, MILP-1 may produce sub-optimal solutions. We use Figure 4 to illustrate it. Figure 4(a) shows a 5-node chain topology and each of the nodes from 1 to 4 generates a flow of same throughput U towards node 5. The number above each link indicates its traffic load. The other assumptions are similar to Figure 2. Figure 4(b) gives an optimal solution where the assigned spectrum exactly matches each link's traffic load and no two links interfere with each other. However, the programming MILP-1 may produce a solution like Figure 4(c) where link (1, 2) and (4, 5) will share a same spectrum segment [30 MHz, 60 MHz]. Under perfect time scheduler, both schemes in Figure 4(b) and 4(c) can get a same throughput of 6 Mbps for every flow. However, when the contention-based MAC technology like IEEE802.11 DCF is used, link (1, 2) will interfere with link (4, 5) in the scheme of Figure 4(c), causing some unnecessary contention and collision, and thus decreasing the network performance. The reason why MILP-1 may produce sub-optimal solution is that its constraints are not able to take the cost of contention and collision into consideration.

The above example suggests that we should select a solution that can minimize interference from all solutions which may be produced by MILP-1, that is, all solutions attaining the same optimal λ valued of λ^*. First we adopt following weighted metric to quantify the total interference.

$$\text{Tot\_Inf}_{(\overline{x},\overline{y},f,\lambda)} = \sum_{(n_p,m_q)\in E'} \left\{ \sum_{(s,d)\in T} \left(f^{s,d}_{n_p,m_q} + f^{s,d}_{m_q,n_p} \right) \cdot \sum_{(u,v)\in Inf(n,m)} \sum_{h,l} I_{n_p,m_q,u_h,v_l} \right\}, \tag{25}$$

where $\sum_{(s,d)\in T}(f^{s,d}_{n_p,m_q} + f^{s,d}_{m_q,n_p})$ is the total traffic over logical link (n_p, m_q) and $\sum_{(u,v)\in \text{Inf}(n,m)} \sum_{h,l} I_{n_p,m_q,u_h,v_l}$ is the number of other logical links interfering with (n_p, m_q).

Then we resolve the programming MILP-1 with the modified goal of minimizing the metric Tot_inf with λ fixed at λ^*, that is, we replace the constraint (13) with the following equality

$$\sum_{m\in\{\nu|(n,\nu)\in E\}} \sum_{p=1}^{K_n} \sum_{q=1}^{K_m} \left(f^{s,d}_{n_p,m_q} - f^{s,d}_{m_q,n_p} \right) = \begin{cases} \lambda^* L_{s,d}, & \text{if } s = n, \\ -\lambda^* L_{s,d}, & \text{if } d = n, \\ 0, & \text{otherwise}, \end{cases} \tag{26}$$

Note that the metric Tot_inf in (25) is nonlinear, but we can easily linearize it via the techniques in Section 5.1 since I_{n_p,m_q,u_h,v_l} is an implied binary variable and $f^{s,d}_{m_q,n_p}$ is a nonnegative real variable with upper bound $\lambda^* l_{s,d}$. Thus the new programming is still a mixed integer linear programming. We call the modified programming MILP-2.

Table 1: Binary linearization techniques.

Nonlinear constraint	Variable Specification	Equivalent linear constraints
$\pi = \theta_1 \times \theta_2$	$\theta_1,\ \theta_2 \in \{0,1\}$	$\theta_1 + \theta_2 - \pi \le 1$ $0 \le \pi \le \theta_1$ $0 \le \pi \le \theta_2$
$\tau = \theta_1 \oplus \theta_2$	$\theta_1,\ \theta_2 \in \{0,1\}$	$\theta_1 - \theta_2 \le \tau$ $\theta_2 - \theta_1 \le \tau$ $\tau \le \theta_1 + \theta_2$ $\tau \le 2 - \theta_1 - \theta_2$
$\sigma = r \times \theta_1$	$\theta_1 \in \{0,1\}$, $r \in \mathbb{R}$, and $0 \le r \le r_{\max}$	$0 \le \sigma \le r_{\max}\theta_1$ $r_{\max}(\theta_1 - 1) + r \le \sigma$ $\sigma \le r_{\max}(1 - \theta_1) + r$

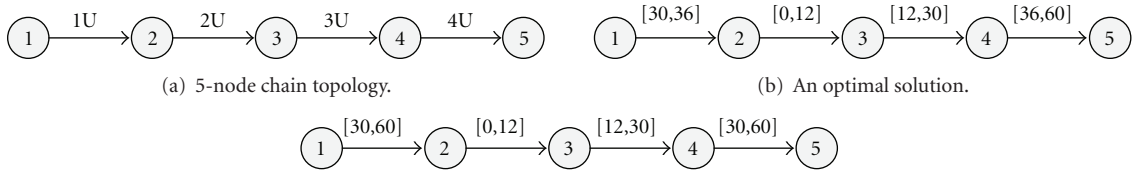

(a) 5-node chain topology.

(b) An optimal solution.

(c) A suboptimal solution which may be produced by MILP-1.

Figure 4: MILP-1 may produce suboptimal solution. We still assume that the total available spectrum is 60 MHz wide and each 1 MHz spectrum can deliver 1 Mbps data rate. Under perfect time scheduler, both schemes in Figures 4(b) and 4(c) can obtain the same throughput U of 6 Mbps for every flow. But in the scheme of Figure 4(c), link (1, 2) interferes with link (4, 5). When the contention-based MAC technology is used, it may cause unnecessary contention and collision.

5.3. Heuristic MILP-based Iterative Local Search Algorithm. It is well known that the computational complexity of a mixed integer linear programming mainly depends on the number of integer variables [23]. So for large-scale networks, it will not be trivial to find the optimal solutions to MILP-1 and MILP-2. So we need to make some tradeoff between the performance improvement and computation complexity. In this section, we present our heuristic suboptimal algorithm.

Our heuristic algorithm is an iterative local search algorithms [26] in which the basic idea is to start with an initial feasible solution and then make modifications to improve its quality using the original MILP. In this section, we only assume that the multipath routing is used, and all nodes are equipped with same K interfaces.

We initially partition the whole available spectrum into K segments with approximately same size. Then we will assign the first $b_{\max}/\omega$ spectrum blocks of each segment to the interfaces of every node. For example, if we have 30 spectrum blocks, and $K = 3$, $b_{\max}/\omega = 6$, we will assign blocks 1-6, blocks 11–16, and blocks 21–26 to the first, second and third interface of every node, respectively. Obviously, the network is full connected and only the logic links in the set $\{(n_i, m_i) | (n,m) \in E, i = 1, \ldots, K\}$ are preserved.

Then we run the programming MILP-1 on the full connected networks under the given initial spectrum assignment to obtain an initial load balance routing. Note here that MILP-1 becomes a linear programming. With the initial spectrum assignment and routing, we will iterate to create a sequence of solutions in an attempt to gradually improve the network performance.

In iteration i, we first sort all logical links (n_p, m_q) in the decreasing order of the following congestion metric:

$$\mathrm{Cong}\left(n_p, m_q\right) = u_{n_p,m_q} + \sum_{(u,v)\in \mathrm{Inf}\,(n,m)} \sum_{h,l} u_{u_h,v_l} I_{n_p,m_q,u_h,v_l}, \tag{27}$$

which is the term on the left-hand side of constraint (22), denoting the congestion status of the collision domain centered at the logical link (n_p, m_q).

We should adopt some randomness to escape from the local optimum. So then we randomly choose a logical link (n_p, m_q) from the L most congested links and try to adjust the spectrum allocation of all interfaces in the interference range of nodes n and m. The adjustment is conducted by running a modified version of MILP-1 and MILP-2, where the variables are only a subset of variables of the original problem, while the values of others are kept as constant as those in the previous iteration. Note only that the variables $\overline{x}, \overline{y}$, f, and λ are what we concern about while others are only intermediate variables. For any radio interface u_h where $\exists v \in V$ that $(u,v) \in \mathrm{Inf}\,(n,m)$, we mark $\overline{x}_{u_h}$, $\overline{y}_{u_h}$ as variables of the new iteration. We also mark $f^{s,d}_{u_h,v_l}$ for all $(u_h, v_l) \in E'$, for all $(s,d) \in T$ to be variables. The modified problem has much fewer integer variables than the original one, so we can solve it easily by branch-and-bound algorithm. It can be viewed as the local search process.

The iteration will terminate when a maximum number $(i_{\max})$ of allowed iterations have passed without improvement. In our algorithms, we set $i_{\max}$ to $2|E|$. A brief description of our algorithms is shown in Algorithm 1.

Input: $G(V, E)$, $b_{\min}$, $b_{\max}$, ω, $\mathcal{F}$, K, c_{unit}
Output: spectrum allocation $\overline{x}$, $\overline{y}$ and routing f
BEGIN
1. Partition the whole available spectrum into K segments with approximately same size.
2. Assign the first $b_{\max}/\omega$ spectrum blocks of each segment to the interfaces of every node.
3. Run the programming MILP-1 on the full connected networks under the given initial spectrum assignment to obtain an initial load balance routing, initial $\lambda^{(0)}$ and $\text{Tot\_inf}^{(0)}$.
4. $i = 0, j = 1$.
5. WHILE $i \le i_{\max}$ DO
   (a) Sort logical links $(n_p, m_q) \in E'$ in the decreasing order of the metric $\text{Cong}(n_p, m_q)$
   (b) Randomly choose a logical link (n_p, m_q) from the L most congested links
   (c) Solve the modified programming MILP-1 with the following variables:
   $$\{\overline{x}_{u_h}, \overline{y}_{u_h} | \exists \nu\ (u, \nu) \in \text{Inf}\ (n, m)\} \cup \{f^{s,d}_{u_h,v_l}(u_h, v_l) \in E', (s, d) \in T\} \cup \{\lambda\}$$
   while the values of others are kept as constant as in previous iteration. The new objective value of MILP-1 is $\lambda^{(j)}$.
   (d) Solve the modified programming MILP-2 with the same set of variables as in step 5(c) while the value of λ is fixed at $\lambda^{(j)}$, and get the new value of total interference $\text{Tot\_inf}^{(j)}$
   (e) IF $\lambda^{(j)} = \lambda^{(j-1)}$ && $\text{Tot\_inf}^{(j)} = \text{Tot\_inf}^{(j-1)}$
   $i = i + 1$.
   END IF
   (f) $j = j + 1$
   END WHILE
END

Algorithm 1: MILP-based Heuristic Iterative Local Search Algorithms.

6. Performance Evaluation

In this section, we compare the performance of our proposed channel width adaptable network architecture with the traditional multi-radio multi-channel networks using fixed-width channels. We also discuss the impact of some system parameters on the network performance.

The simulation is conducted by NS-2 simulator [27]. We use the methods described in [28] to add multi-interface support and extend the channel module to enable channel width adaptation. The following are the *default* settings for simulation. We use IEEE802.11 DCF as the MAC layer, and RTS/CTS mechanism is enabled. The two-ray propagation model is used to model the path loss. The transmission range is set to be 250 m, and the interference range is 550 m. The total available spectrum is assumed to be 120 MHz-wide, and each node is equipped with three interfaces. For our channel width adaptable architecture, we set the default spectrum block size ω to be 5 MHz, and set $b_{\min}$ and $b_{\max}$ to be 5 MHz and 50 MHz respectively. The *default* routing scheme is multi-path routing. In our implementation of the multipath routing in NS-2, every node forwards data packets across different links with the probability proportional to the routing flows calculated by our programming.

6.1. Optimal and Suboptimal Solutions on Grid Topology. We first present the results obtained by the optimal branch-and-cut solver [25] and our heuristic MILP-based iterative local search algorithm on the 6×6 grid topology. We also investigate the performance of MR-MC networks using fixed-width channels, whose solution can be obtained from our MILP programming by adding the constraint $b_{\min} = b_{\max} = 20$ MHz. We repeat our simulation on the 6×6 grid topology for 10 randomly generated traffic profiles. In each profile, we randomly chose twelve source and destination node pairs to generate UDP (User Datagram Protocol) sessions. Each has the transmission demand uniformly distributed between 1 Mbps and 5 Mbps. Then we change every flow's rate proportionally until the network can satisfy 90% of the injected traffic. The metric we examine is the total useful throughput across all sessions.

Figure 5 shows the total useful throughput obtained by the optimal solution, our heuristic solution, and the case using fixed-width channels. It shows that in the grid topology, the optimal solution can outperform the case using fixed-width channels by 32% on average while our heuristic algorithm can improve the performance by 24% on average. The performance gap between the optimal solution and our heuristic solution is about 8%.

6.2. Comparison with "Hyacinth" Architecture. "Hyacinth" is a typical MR-MC mesh networks. A static centralized fixed-width channel assignment algorithm for "Hyacinth" architecture is proposed in [8]. With the assumption that most traffic is between the mesh clients and the gateway nodes, it first estimates the total expected load on each virtual link by summing the load due to each offered traffic flow. Then, the channel assignment algorithm visits each virtual link in decreasing order of expected traffic load and greedily assigns it a channel. In this subsection, we compare the performance of our heuristic channel-width adaptation algorithm with the typical WMN architecture "Hyacinth." In "Hyacinth" architecture, we want to study the impact

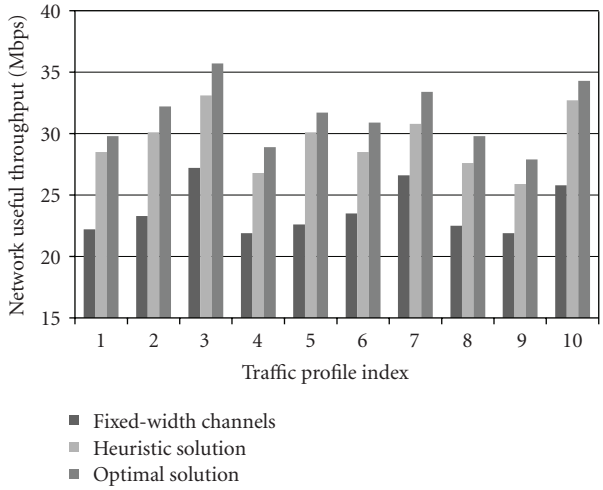

Figure 5: Comparison on the total useful throughput of the optimal solution and heuristic solution across 10 traffic profiles.

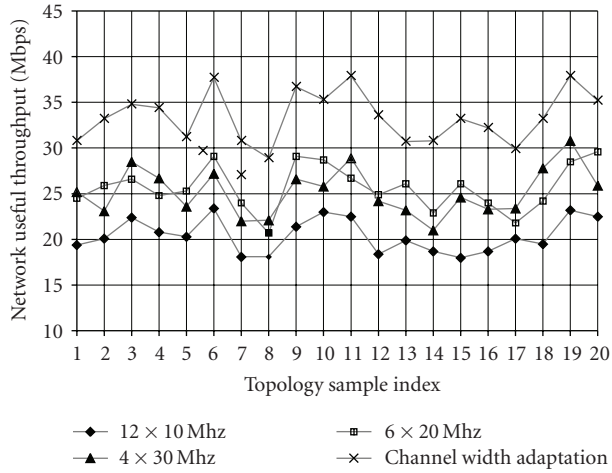

Figure 6: Comparison on the total useful throughput between Hyacinth and our algorithm across 20 randomly generated topologies.

of different static spectrum partition styles. Specifically, three cases are investigated: (1) The 120 MHz-wide available spectrum is divided into twelve 10 MHz-wide channels. (2) Six 20 MHz-wide channels and (3) Four 30 MHz-wide channels.

The simulation scenario is an area of 1000 m×1000 m consisting of 40 randomly located mesh nodes. Among the 40 nodes, 3 nodes are randomly chosen to act as gateways and 15 nodes are chosen to generate UDP traffic flows towards one of these gateway nodes. The initial rate of traffic flow is also uniformly selected between 1 Mbps and 5 Mbps. Remaining nodes only act as traffic routers. We proportionally change every flow's rate until the network can satisfy 90% of the traffic. In this subsection, both the "Hyacinth" architecture and our algorithms adopt the single-path routing.

Figure 6 shows the total useful throughput of the above three static spectrum partition styles and our heuristic algorithm in twenty randomly generated topologies. The case of 12 × 10 MHz-wide channels usually performs the worst since the number of interfaces constraints the maximal spectrum resource that a node can utilize. In this case, even though all interfaces are saturated, some portion of the spectrum is still not utilized. For the case of 4 × 30 MHz-wide channels and the case of 6 × 20 MHz-wide channels, we find that no one can dominate the other across all topologies because different topologies and traffic profiles give different preferences to spectrum partition styles. By adjusting channel width to cater to different topology and traffic demand, our scheme always outperforms the others and get an improved total throughput by 18% to 46% compared with the cases of 4×30 MHz and 6×20 MHz. Note the performance improvements are achieved without using extra spectrum resources. Thus, the spectrum is utilized more efficiently in our architecture. The key reason is that we can distribute the load across the spectrum as evenly as possible, and links can share the spectrum resource in a much fairer way than in static spectrum partition styles. And by creating many small-width channels, the phenomena of collision, contention, and interference among links can be significantly reduced or even eliminated, and thus the performance is further improved.

6.3. The Impact of Spectrum Block Size. The most important system parameter in our algorithms is the size of spectrum block ω. With small spectrum block size, we can adjust channel width in a finer granularity and it is possible to obtain more performance improvement. However, using too small spectrum block size will incur significant hardware cost and computation complexity. In this subsection we investigate the impact of spectrum block size ω on the network performance.

The simulation scenario is similar to that of Section 6.2. We vary the spectrum block size ω from 1 MHz to 15 MHz. The MR-MC networks using 6 × 20 MHz-wide channels is used as the comparison baseline. Figure 7 shows the relative performance gains under different spectrum block size. Each point is the average of measurements for twenty randomly generated topologies. Generally speaking, the performance gain is increased as the spectrum block size becomes small. But when the spectrum block size $\omega \geq 10$ MHz, there is nearly no improvement compared with the case using fixed-width channels. And when $\omega < 4$ MHz, the improvement due to using much smaller spectrum block will become unremarkable. So some tradeoff should be made between the hardware complexity and performance improvement. We may think 5 MHz is the most appropriate spectrum block size for our simulation scenario.

6.4. The Impact of Routing Scheme. In this subsection, we investigate the impact of routing scheme on the network performance with or without channel width adaptation. Specifically, four cases are investigated: Multi-path routing combined with Fixed-width Channels (MP-FC), Multi-path routing with channel Width Adaptation (MP-WA), Single-path routing with Fixed-width Channels (SP-FC),

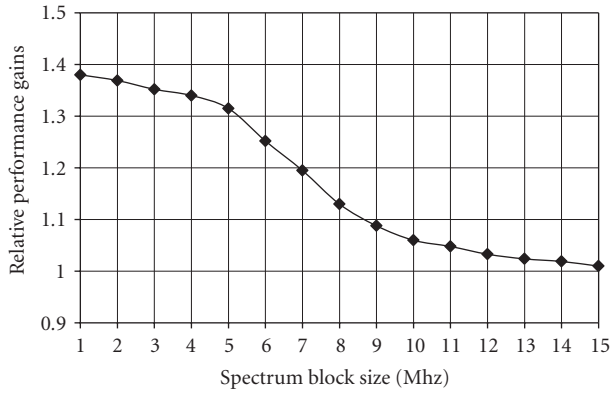

Figure 7: Comparison of the performance gains under different spectrum block size.

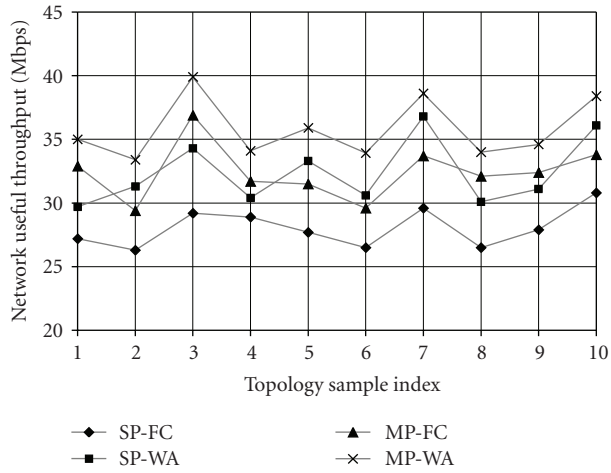

Figure 8: Comparison on the total useful throughput under different routing schemes across 10 randomly generated topologies.

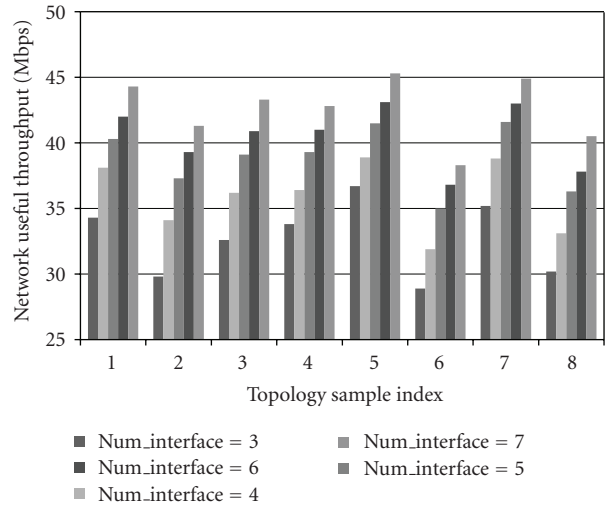

Figure 9: Comparison on the total useful throughput using different number of interfaces across 8 randomly generated topologies.

and Single-path routing with channel Width Adaptation (SP-WA). For the cases of fixed-width channels, the whole available spectrum is divided into six 20 MHz-wide non-overlapped channels. Figure 8 shows the total useful throughput for the four cases across ten randomly generated topologies. As we can expect, SP-FC usually performs worst while MP-WA always performs best. And for the cases of MP-FC and SP-WA, no one can dominate the other across all topologies. Actually multipath routing and channel width adaptation are complementary to each other. Multi-path routing takes advantage of load balancing across links, while channel width adaptation can distribute the load more evenly across spectrum.

6.5. The Impact of Number of Interfaces per Node. In multi-radio multi-channel mesh networks using fixed-width channels, there is no need to equip each node with more interfaces than the number of channels. However, with the ability of channel width adaptation, we can benefit from equipping more interfaces in our architecture. Figure 9 shows the effect of varying number of interfaces per node on network throughput. The useful throughput increases monotonically with the number of interfaces. And even when the number of interfaces exceeds 6, some performance gains still can be obtained, though at this time the values of λ calculated in our programming are almost same (note that the values of λ indicates the *upper bound* of the network capacity). This is because with more interfaces, it is possible to create more small-width channels, thus reducing interference among links and saving the spectrum resource from contention and collision. It can also mitigate the problem of spectrum overfragmentation and thus the spectrum can be more efficiently utilized.

7. Conclusion

In this paper, we address how to adapt channel width to make full use of the spectrum resource in multi-radio multi-channel wireless mesh networks. We mathematically formulate the channel width adaptation, topology control and routing as the mixed 0-1 integer linear optimization. We also propose a heuristic assignment algorithm. Simulation results show that our algorithm can significantly improve spectrum use efficiency and network performance.

Our work distinguishes from prior optimization works in that it does not treat the spectrum as the set of discrete orthogonal channels but the continuous resource. The combination of variable channel widths and center frequencies offers rich possibilities for improving system performance. A lot of things still need to be done. Currently, we are exploiting the partially overlapped channels with adaptable widths in our model to further improve the spectrum efficiency.

References

[1] I. F. Akyildiz, X. Wang, and W. Wang, "Wireless mesh networks: a survey," *Computer Networks*, vol. 47, no. 4, pp. 445–487, 2005.

[2] P. Gupta and P. R. Kumar, "The capacity of wireless networks," *IEEE Transactions on Information Theory*, vol. 46, no. 2, pp. 388–404, 2000.

[3] IEEE 802.11b Standard, http://standards.ieee.org/getieee802/802.11.html.

[4] R. Chandra, R. Mahajan, T. Moscibroda, R. Raghavendra, and P. Bahl, "A case for adapting channel width in wireless networks," in *Proceedings of the ACM SIGCOMM Conference on Data Communication*, pp. 135–146, Seattle, Wash, USA, August 2008.

[5] T. Moscibroda, R. Chandra, Y. Wu, S. Sengupta, P. Bahl, and Y. Yuan, "Load-aware spectrum distribution in wireless LANs," in *IEEE International Conference on Network Protocols (ICNP '08)*, pp. 137–146, Orlando, Fla, USA, October 2008.

[6] Y. Yuan, P. Bahl, R. Chandra, T. Moscibroda, and Y. Wu, "Allocating dynamic time-spectrum blocks in cognitive radio networks," in *Proceedings of the 8th ACM International Symposium on Mobile Ad Hoc Networking and Computing (MobiHoc '07)*, pp. 130–139, Montreal, Canada, September 2007.

[7] I. F. Akyildiz, W.-Y. Lee, M. C. Vuran, and S. Mohanty, "NeXt generation/dynamic spectrum access/cognitive radio wireless networks: a survey," *Computer Networks*, vol. 50, no. 13, pp. 2127–2159, 2006.

[8] A. Raniwala, K. Gopalan, and T. Chiueh, "Centralized channel assignment and routing algorithms for multi-channel wireless mesh networks," *ACM SIGMOBILE Mobile Computing and Communications Review*, vol. 8, no. 2, pp. 50–65, 2004.

[9] A. Raniwala and T.-C. Chiueh, "Architecture and algorithms for an IEEE 802.11-based multi-channel wireless mesh network," in *Proceedings of the 24th IEEE Annual Joint Conference of the IEEE Computer and Communications Societies (INFOCOM '05)*, vol. 3, pp. 2223–2234, Miami, Fla, USA, March 2005.

[10] J. Tang, G. Xue, and W. Zhang, "Interference-aware topology control and QoS routing in multi-channel wireless mesh networks," in *Proceedings of the 6th ACM International Symposium on Mobile Ad Hoc Networking and Computing (MobiHoc '05)*, pp. 68–77, Urbana-Champaign, Ill, USA, May 2005.

[11] P. Kyasanur and N. H. Vaidya, "Routing and interface assignment in multi-channel multi-interface wireless networks," in *Proceedings of the IEEE Wireless Communications and Networking Conference (WCNC '05)*, vol. 4, pp. 2051–2056, New Orleans, La, USA, March 2005.

[12] R. Draves, J. Padhye, and B. Zill, "Routing in multi-radio, multi-hop wireless mesh networks," in *Proceedings of the 10th Annual International Conference on Mobile Computing and Networking (MOBICOM '04)*, pp. 114–128, Philadelphia, Pa, USA, September 2004.

[13] M. Alicherry, R. Bhatia, and L. Li, "Joint channel assignment and routing for throughput optimization in multi-radio wireless mesh networks," in *Proceedings of the 11th Annual International Conference on Mobile Computing and Networking (MOBICOM '05)*, pp. 58–72, Cologne, Germany, August-September 2005.

[14] M. Kodialam and T. Nandagopal, "Characterizing the capacity region in multi-radio multi-channel wireless mesh networks," in *Proceedings of the 11th Annual International Conference on Mobile Computing and Networking (MOBICOM '05)*, pp. 73–87, Cologne, Germany, August-September 2005.

[15] A. K. Das, H. M. K. Alazemi, R. Vijayakumar, and S. Roy, "Optimization models for fixed channel assignment in wireless mesh networks with multiple radios," in *Proceedings of the 2nd Annual IEEE Communications Society Conference on Sensor and AdHoc Communications and Networks (SECON '05)*, pp. 463–474, Santa Clara, Calif, USA, September 2005.

[16] A. H. M. Rad and V. W. S. Wong, "WSN16-4: logical topology design and interface assignment for multi-channel wireless mesh networks," in *Proceedings of the IEEE Global Telecommunications Conference (GLOBECOM '06)*, pp. 1–6, San Francisco, Calif, USA, November-December 2006.

[17] Y. T. Hou, Y. Shi, and H. D. Sherali, "Optimal spectrum sharing for multi-hop software defined radio networks," in *Proceedings of the 26th IEEE Annual Joint Conference of the IEEE Computer and Communications Societies (INFOCOM '07)*, pp. 1–9, Anchorage, Alaska, USA, May 2007.

[18] T. M. Cover and J. A. Thomas, *Elements of Information Theory*, John Wiley & Sons, New York, NY, USA, 1991.

[19] J. Tang, G. Xue, and W. Zhang, "Maximum throughput and fair bandwidth allocation in multi-channel wireless mesh networks," in *Proceedings of the 25th IEEE Conference on Computer Communications (INFOCOM '06)*, pp. 1–10, Barcelona, Spain, April 2006.

[20] F. Glover and E. Woolsey, "Further reduction of zero-one polynomial programming problems to zero-one linear programming," *Operations Research*, vol. 21, no. 1, pp. 156–161, 1973.

[21] C.-T. Chang and C.-C. Chang, "A linearization method for mixed 0-1 polynomial programs," *Computers & Operations Research*, vol. 27, no. 10, pp. 1005–1016, 2000.

[22] A. H. M. Rad and V. W. S. Wong, "Partially overlapped channel assignment for multi-channel wireless mesh networks," in *Proceedings of the IEEE International Conference on Communications (ICC '07)*, pp. 3770–3775, Glasgow, UK, June 2007.

[23] S. G. Nash and A. Sofer, *Linear and Nonlinear Programming*, McGraw-Hill, Boston, Mass, USA, 1996.

[24] "LINDO MILP solver," http://www.lindo.com.

[25] ILOG CPLEX, http://www.ilog.com/products/cplex.

[26] H. R. Lourenco, O. Martin, and T. Stutzle, "Iterated local search," in *Handbook of Metaheuristics*, F. Glover and G. Kochenberger, Eds., pp. 321–353, Kluwer Academic Publishers, Dordrecht, The Netherlands, 2002.

[27] UCB/LBNL/VINT, "Network Simulator (ns), version 2," http://www.isi.edu/nsnam/ns.

[28] R. A. Calvo and J. P. Campo, "Adding Multiple Interface Support in NS-2," January 2007, http://personales.unican.es/aguerocr/files/ucMultiIfacesSupport.pdf.